# 12-kW Advanced Electric Propulsion System Hall Current Thruster Qualification and Production Status

Rohit Shastry\*<sup>1</sup>, Hani Kamhawi<sup>2</sup>, Jason D. Frieman<sup>3</sup>, George C. Soulas<sup>4</sup>, Timothy G. Gray<sup>5</sup>, Timothy R. Verhey<sup>6</sup>, Clayton D. Kachele<sup>7</sup>, and George J. Williams<sup>8</sup>

NASA Glenn Research Center, Cleveland, OH, 44135 USA

Nagual A. Simmons<sup>9</sup> *HX5, NASA Glenn Research Center, Cleveland, OH 44135 USA* 

Robert B. Lobbia<sup>10</sup>, Steven M. Arestie<sup>11</sup>, and Vernon H. Chaplin<sup>12</sup> *Jet Propulsion Laboratory, California Institute of Technology, Pasadena, CA 91109 USA* 

Jack Fisher<sup>13</sup>, Gabriella Blackner<sup>14</sup>, Eleanor Forbes<sup>15</sup>, Jack Hondagneu<sup>16</sup>, Nicholas A. Branch<sup>17</sup>, Jonathan M. Zubair<sup>18</sup>, and Hannah Watts<sup>19</sup> *Aerojet Rocketdyne, Redmond, WA, 98052 USA* 

# Acknowledgments

Countless people contributed to the work on the AEPS project presented in this paper, and unfortunately, they cannot all be listed here. However, the authors would be remiss if they did not acknowledge the contributions of the following team members. The authors would like to thank Matt Baird, Drew Ahern, Jon Mackey, Wensheng Huang, Glenda Yee, Jim Gilland, Konrad Shire and Abbey Mattingly for their help in executing the tests and reducing data on QM1 at GRC, Kevin Rahill, Cody Drum, Chad Joppeck, Josh Gibson, Kevin Blake, Zeyad Nooman, and Jim Szelagoski for their support in preparing test hardware, GSE and VF-5 for testing at GRC, and Greg Fedor, Trish Seaman, and Bennett Straker for their quality, safety and mission assurance support during all testing. The authors would like to also thank Anna Sheppard, Eric Smith and Nowell Niblett for their help in executing the component and cathode testing at JPL, and Matthew Byrne for his help in executing the LIF test campaign on TDU-2 at JPL. Lastly, the authors would like to thank Nicolas Rongione, Ethan Dale, Mariah Tunstall, Jeff Asher, Anirudh Thuppul, Angelica Ottaviano, William Cox, and Mark Crofton at The Aerospace Corporation for supporting the AEPS ETU-2 radiated emissions test by acquiring and reporting the radiated emissions data and operating TAC's EP3 vacuum facility; the contributions of John Yim and Corey Rhodes of GRC in support of executing the AEPS test at TAC are also acknowledged. A portion of the research was carried out at the Jet Propulsion Laboratory, California Institute of Technology, under a contract with the National Aeronautics and Space Administration (80NM0018D0004). The AEPS contract is managed by the Solar Electric Propulsion (SEP) project

<sup>\*</sup> Correspondence: rohit.shastry@nasa.gov

<sup>&</sup>lt;sup>1</sup> Solar Electric Propulsion Product Lead Engineer, Electric Propulsion Systems Branch, MS 301-3.

<sup>&</sup>lt;sup>2</sup> Solar Electric Propulsion Thruster Lead, Electric Propulsion Systems Branch, MS 301-3.

<sup>&</sup>lt;sup>3</sup> Solar Electric Propulsion Deputy Thruster Lead, Electric Propulsion Systems Branch, MS 301-3.

<sup>&</sup>lt;sup>4</sup> Solar Electric Propulsion GRC Test Lead, Electric Propulsion Systems Branch, MS 301-3.

<sup>&</sup>lt;sup>5</sup> Solar Electric Propulsion Deputy Product Lead Engineer, Electric Propulsion Systems Branch, MS 301-3.

<sup>&</sup>lt;sup>6</sup> Solar Electric Propulsion Cathode Lead, Electric Propulsion Systems Branch, MS 301-3.

<sup>&</sup>lt;sup>7</sup> Solar Electric Propulsion Project Manager, Space Technology Project Office.

<sup>&</sup>lt;sup>8</sup> Solar Electric Propulsion Deputy Project Manager, Space Technology Project Office.

<sup>&</sup>lt;sup>9</sup> Solar Electric Propulsion Cathode Test Engineer, Electric Propulsion Systems Branch, MS 301-3.

<sup>&</sup>lt;sup>10</sup> Solar Electric Propulsion JPL Test Lead.

<sup>&</sup>lt;sup>11</sup> Solar Electric Propulsion Component Test Lead.

<sup>&</sup>lt;sup>12</sup> Solar Electric Propulsion Test Engineer.

<sup>&</sup>lt;sup>13</sup> Advanced Electric Propulsion System Program Manager, Aerojet Rocketdyne.

<sup>&</sup>lt;sup>14</sup> Advanced Electric Propulsion System Chief Engineer, Aerojet Rocketdyne.

<sup>&</sup>lt;sup>15</sup> Advanced Electric Propulsion System Technical Lead, Aerojet Rocketdyne.

<sup>&</sup>lt;sup>16</sup> Advanced Electric Propulsion System Test Engineer, Aerojet Rocketdyne.

<sup>&</sup>lt;sup>17</sup> Advanced Electric Propulsion System Senior Test Engineer, Aerojet Rocketdyne

<sup>&</sup>lt;sup>18</sup> Advanced Electric Propulsion System Senior Test Engineer, Aerojet Rocketdyne

<sup>&</sup>lt;sup>19</sup> Advanced Electric Propulsion System Test Engineer, Aerojet Rocketdyne.

at NASA GRC under the Technology Demonstration Missions program as a part of NASA's Space Technology Mission Directorate, with AR being funded under contract # NNC16CA21C.

#### Abstract

Initial developments by the National Aeronautics and Space Administration (NASA) of a 12-kW-class Hall thruster began with maturation of the Hall Effect Rocket with Magnetic Shielding, which was then transitioned to industry via the Advanced Electric Propulsion System contract. This contract was awarded to Aerojet Rocketdyne (now part of L3Harris) in 2016 with the goal of developing and fully qualifying a 12 kW Hall thruster for NASA and commercial applications, with its first intended use on the Power and Propulsion Element as part of NASA's Gateway lunar space station. This paper describes the status of the contract, including production and qualification efforts after the thruster design successfully passed Critical Design Review in 2022, as well as NASA-led independent testing in support of development and qualification. To-date, the first qualification thruster has successfully undergone pre-environmental characterization testing, qualification vibration and shock testing, with preparations for thermal vacuum testing underway at time of writing. Additional qualification testing of components such as the cathode, magnet coils, and thermal components are ongoing to demonstrate design robustness of these critical thruster elements. Flight hardware fabrication and testing is expected to be completed by 2025, at which point the hardware will be delivered to Maxar Technologies for integration and use on the Power and Propulsion Element spacecraft.

#### **Declarations**

## **Funding**

This work was jointly funded by the Technology Demonstration Missions program as part of NASA's Space Technology Mission Directorate, as well as NASA's Exploration Systems Development Mission Directorate via the Power and Propulsion Element project, with Aerojet Rocketdyne being funded under contract # NNC16CA21C.

## **Conflicts of interest/Competing interests**

The authors have no competing interests to declare that are relevant to the content of this article.

#### Data availability

Qualification model characterization data presented in Figures 9 and 11, as well as ion temperature data in Figures 17 and 18 within the manuscript are available upon reasonable request.

#### Code availability

Not applicable

#### Authors' contributions

All authors contributed to the execution and/or oversight of the work described in this manuscript. Hani Kamhawi, Jason Frieman, Nagual Simmons, Vernon Chaplin, and authors from Aerojet Rocketdyne wrote various sections, while Rohit Shastry was responsible for integration of the manuscript as well as presentation of the work at IEPC.

## 1.0 Motivation and Background

NASA continues to evolve a human exploration approach for beyond low-Earth orbit and to do so, where practical, in a manner involving international, academic, and industry partners. The center of this approach is NASA's Gateway that is envisioned to provide a maneuverable outpost in lunar orbit that extends human presence in deep space and expands on NASA's exploration goals. The Gateway represents the initial step in NASA's architecture for human cislunar operations, lunar surface access, and missions to Mars.

NASA announced at the May 2020 NASA Advisory Council's Human Explorations and Operations Committee a plan that calls for launching the first two elements of Gateway as a co-manifested mission. Launching the Power and Propulsion Element (PPE) and the Habitation and Logistics Outpost (HALO) together reduces mission risk, utilizes PPE's high-power Solar Electric Propulsion (SEP) system to transport both elements to lunar orbit, and reduces overall cost. NASA has partnered with Maxar Space Systems to build the PPE while leveraging their existing commercial spacecraft platform and technical expertise. The PPE will utilize a 48-kW electric propulsion system comprised of three 12-kW Advanced Electric Propulsion System (AEPS) Hall thrusters developed and supplied by Aerojet Rocketdyne (AR) and four 6-kW Hall thrusters.

Development of the 12-kW Hall thruster electric propulsion system was led by the NASA Glenn Research Center

(GRC) and the Jet Propulsion Laboratory (JPL) and began with maturation of the Hall Effect Rocket with Magnetic Shielding (HERMeS) Technology Demonstration Units (TDUs). Technology development transitioned to AR via the AEPS contract, which is managed by NASA GRC with funding from NASA's Space Technology Mission Directorate under the Technology Demonstration Missions Program.

# 2.0 **AEPS Project Overview**

The AEPS contract was awarded to AR in May of 2016 with the goal of developing a 12.5kW Hall Thruster System, including the Hall Current Thruster (HCT), Power Processor Unit (PPU) and Xenon Flow Controller (XFC). It was originally targeted to support the Asteroid Redirect Mission, which was cancelled early in the project. The project was subsequently restructured to support the Gateway PPE propulsion mission, with modified scope that consisted of the development, qualification and delivery of three 12kW flight thrusters. The PPU and XFC components were designed and development hardware fabricated with initial testing performed prior to being de-scoped from the contract. System level testing was performed by AR using these engineering components in early 2022 at the Aerospace Corporation's EP-3 test facility [1].

The AEPS project was structured to include all appropriate critical check points and formal review meetings, consisting of:

- System Requirement Reviews (SRR)
- Preliminary Design Review (PDR)
- Critical Design Review (CDR)
- Production Readiness Review (PRR)
- Test Readiness Reviews (TRR) Multiple meetings held for both qualification and flight hardware
- Qualification Subsystem Acceptance Reviews (QSAR) One for each qualification thruster
- System Acceptance Reviews (SAR) One for each flight thruster

The project has progressed through the development, qualification and flight manufacturing phases from 2016 through early 2024, as shown in Fig. 1 below.

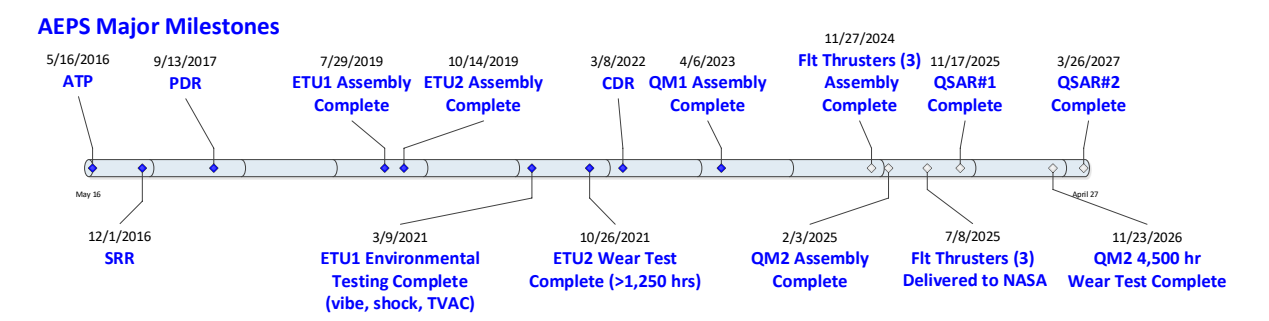


Fig. 1 Timeline of AEPS project illustrating key milestones

AR based the design of the AEPS thruster on the HERMeS thruster, with substantial modifications to improve manufacturability, structural robustness, cycle life capability and ease of spacecraft integration. A pair of Engineering Test Unit (ETU) thrusters, as well as several individual thruster components, were fabricated early in the project and underwent an extensive development test campaign that encompassed all test phases planned for qualification including detailed performance assessments, wear tests, and environmental testing (i.e., vibration, shock, and thermal vacuum cycling). Between testing of the HERMeS TDUs and AEPS ETUs, over 8,000 h of development testing was completed on the 12-kW Hall thruster. The successful completion of this development campaign reduced the risk of AEPS design compliance with thruster requirements and enabled AEPS to successfully complete its CDR in March 2022.

Since CDR, AR has successfully completed assembly and acceptance testing of the first qualification thruster, designated QM1, in 2023 (see Fig. 2). This thruster has subsequently completed pre-environmental hot fire characterization, qualification level vibration and mechanical shock testing, and



**Fig. 2** AEPS Qualification Thruster Model #1 (QM1) at final assembly

is currently being prepared for TVAC testing. The second qualification thruster, designated QM2, is approaching final assembly and will be used to support the planned 4,500 h wear test. After completion of 4,500 h of operation by AR, NASA will continue the wear test to demonstrate full lifetime capability up to 23,000 h.

Flight thrusters are at various stages of final/subassembly (see Fig. 3) and are projected to enter acceptance testing later this summer, with deliveries completed in 2025.

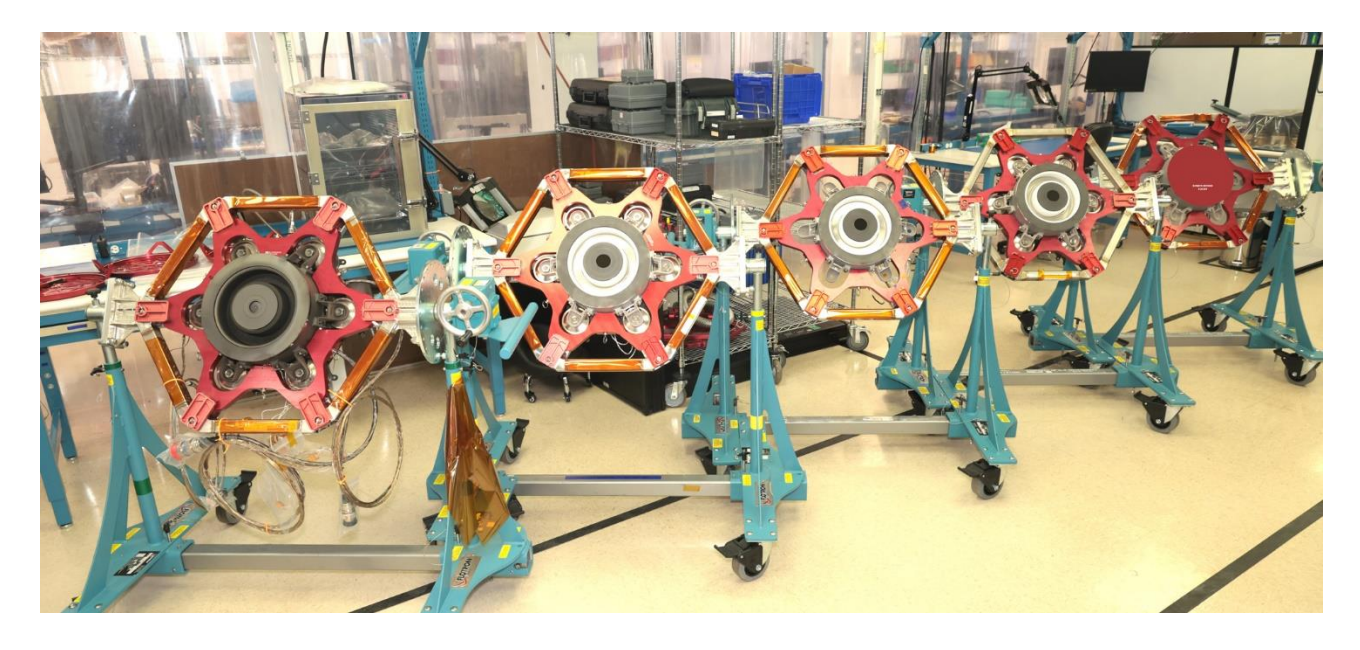


Fig. 3 AEPS qualification and flight thrusters at Aerojet Rocketdyne in Redmond, WA

This paper summarizes the status of the AEPS project, including summaries of both development and qualification hardware testing performed with the thruster and subassemblies, as well as results of integrated system testing.

#### 3.0 AEPS Thruster Design

The AEPS Hall effect thruster has four fundamental subassemblies that work together to achieve the Hall current working mechanism: the discharge chamber, anode assembly, magnetic circuit assembly and cathode assembly. The magnetic field captures electrons produced by the cathode assembly, thereby ionizing neutral xenon that is distributed into the discharge chamber by the gas distributor anode assembly. The ionized xenon is propelled into space by the electric field produced by an electrically biased anode assembly and a negatively charged cathode assembly. Thrust is imparted to the spacecraft by the reaction of the ionized xenon with the magnetic field.

The thruster is designed to be directly mounted to the spacecraft interface with a mounting structure interface. The thruster isolates the thruster body from spacecraft mechanical and electrical interfaces with the use of six shock isolators on the thruster mounting structure. This enables the thruster to be affixed to the spacecraft without a structural adapter. The overall envelope of the thruster is 210mm in height by 530mm in diameter, with a total mass of 53kg.

Three harness assemblies interface to spacecraft power, rated to withstand high radiation and electromagnetic environments that can be routed along the exterior spacecraft surface without additional shielding. The Discharge Cable Assembly provides 300-600V, 10-20A power to the anode, depending on desired operating setpoint. The Auxiliary Cable Assembly provides 50-100V, 2-5A of power to the cathode and magnet components. The Thermal Cable Assembly provides a maximum of 100W to the magnet heaters and temperature sensors. Two propellant line interfaces are used to deliver xenon to the spacecraft, one for the anode and one for the cathode.

The AEPS thruster is the highest power electric propulsion device in production, providing around 600mN of thrust and a specific impulse of around 2800s at a 12kW operating point. This is a mid-range level performance for low thrust, high efficiency electric propulsion technology, offering the benefit of higher relative thrust with a more efficient propellant utilization (see Fig. 4). The AEPS thruster is a throttle-able technology from 300V, 6kW to 600V, 12kW to suit different mission profile and spacecraft design needs.

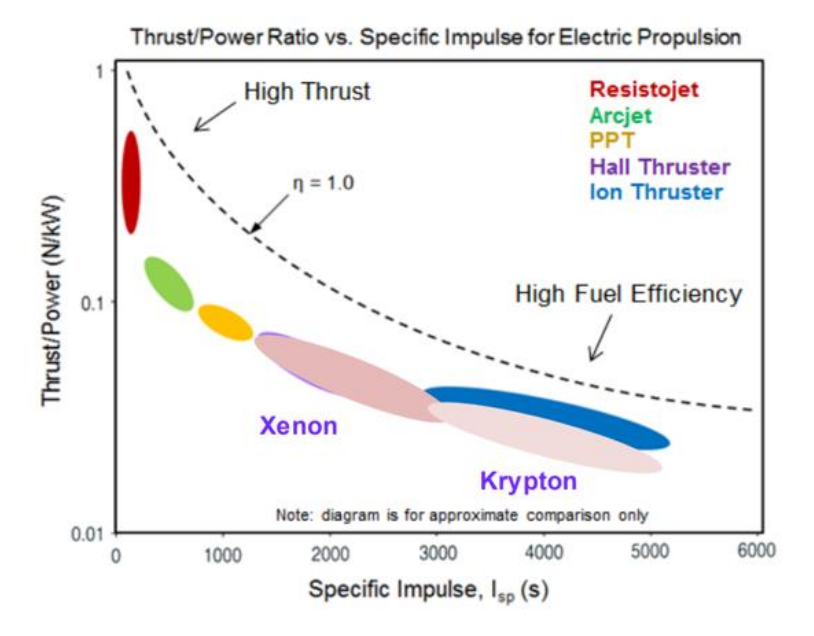
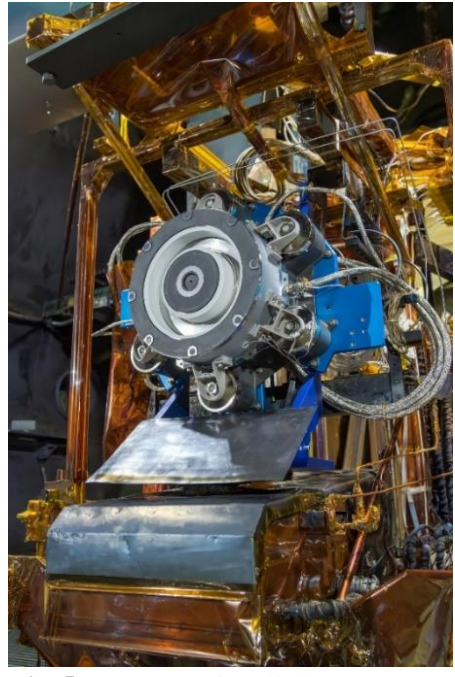


Fig. 4 Electric propulsion performance profiles

## 4.0 AEPS Qualification Approach

After CDR, AR produced the first AEPS Qualification Model (QM1) thruster, which is shown in Fig. 5. QM1 was subjected to an acceptance test program (ATP) and then began its qualification test program (QTP) in 2023 including flow uniformity, hot fire characterizations, random and sine vibration, shock, and thermal vacuum testing. Consistent with ETU testing, all test phases are a collaborative effort led by AR and executed to their test plans and procedure with NASA support. In addition to QM1, AR has also fabricated a qualification cathode which, beginning in 2023, will undergo separate vibration, shock and thermal vacuum tests, as well as life cycle testing. Additional components including the magnet coils, magnet survival heaters, cathode heaters, and temperature sensors will also undergo separate qualification thermal vacuum and life cycle testing as part of the overall qualification effort.

In addition to qualification testing led by AR, a number of independent risk reduction and characterization tests were conducted by NASA in support of the AEPS project. In particular, electromagnetic interference (EMI) characterization of the ETU-2 development thruster was conducted at the Aerospace Corporation in 2023 to aid in spacecraft design and ensure no interferences occur with PPE communications. This test was also conducted with development units of the PPU and XFC provided by Maxar. Risk reduction testing was conducted with the TDU-2 thruster by JPL to measure the presence of lower hybrid waves in support of ongoing thruster life modeling activities. Lastly, risk reduction testing is being performed by GRC on an EDU development cathode to investigate the performance and lifetime impacts of extended atmospheric exposure.



**Fig. 5** AEPS QM1 installed at VF-5 at NASA GRC

The status and results to-date of AR-led AEPS qualification tests are summarized in Section 5.0, while status and results of NASA-led independent testing are summarized in Section 6.0.

# 5.0 Status of AEPS Qualification Testing

#### 5.1 QM1 Thruster Acceptance Testing

Following thruster assembly, QM1 was subjected to the ATP sequence shown in Fig. 6. The overall goals of ATP were to screen for build defects, ensure that the thruster was built per design, and validate thruster performance against the AEPS requirements.

QM1 ATP began with acceptance-level vibration testing, which was conducted at AR's site in Redmond, Washington. In this test phase, QM1 was subjected to both random and sinusoidal vibration in all three axes. Given that the goal of this test was to screen for structural build defects, the levels used during acceptance vibration were reduced to approximately 70-75% of those used for AEPS qualification. Low-level sinusoidal vibration sweeps performed before and after acceptance vibration of each axis as well as detailed electrical health checks (e.g., continuity and isolation resistance) performed before and after the whole acceptance vibration sequence verified that QM1 exhibited no change in structural and electrical characteristics due to exposure to acceptance-level vibration and was therefore compliant with the AEPS structural design.

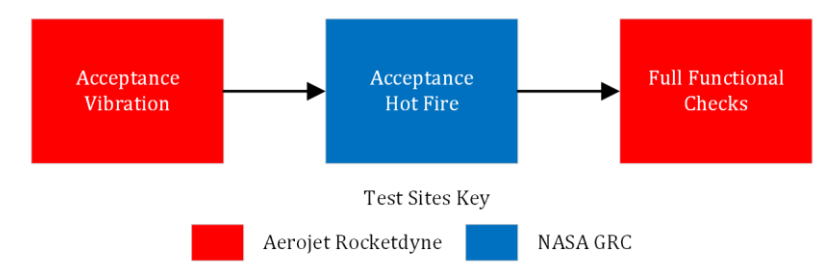


Fig. 6 QM1 ATP test sequence, indicating the location of each test

Following acceptance vibration, QM1 underwent hot fire testing in Vacuum Facility 5 (VF-5) at NASA GRC. This test sequence was performed in the same test facility (i.e., VF-5) and with the same ground support equipment used throughout AEPS development testing and therefore offered a direct comparison of QM1 operating properties to those of the development units [2-4]. The hot fire test began with a set of conditioning sequences intended to ensure that all volatiles had been outgassed from QM1 prior to assessing thruster performance. An image of this first operation of QM1 is shown in Fig. 7.

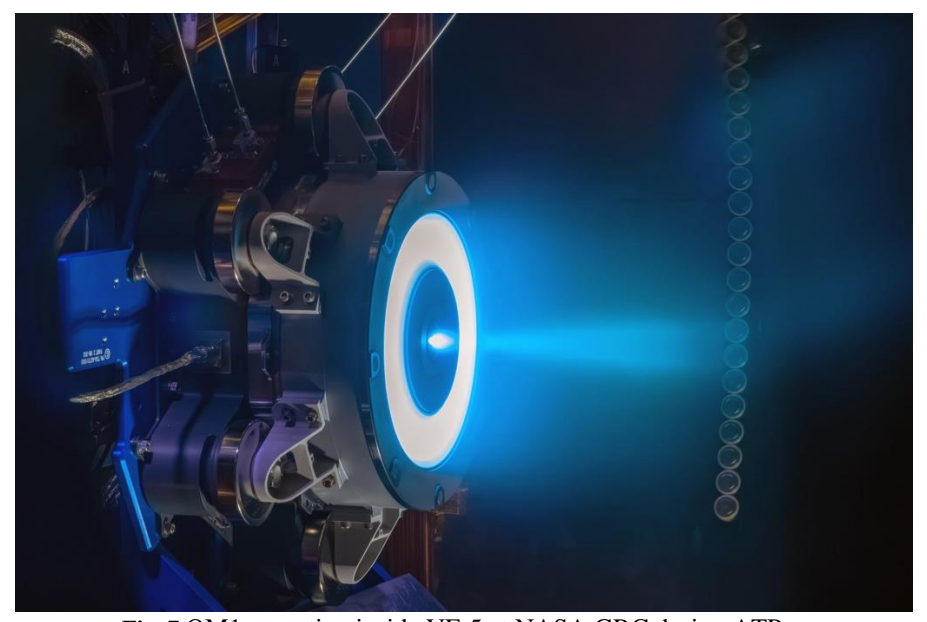


Fig. 7 QM1 operating inside VF-5 at NASA GRC during ATP

Next, QM1 was subjected to an acceptance thermal cycle in which the thruster's on-board thermal control components were demonstrated by cooling the thruster to the heater activation set point and then confirming each heater's ability to activate and warm the thruster using ground support equipment simulating the spacecraft temperature controller. QM1 was then cooled back to the heater activation temperature and ignited to simulate a cold ignition. After the cold ignition, the thruster was operated at the full power condition (600 V/12 kW) until it achieved thermal steady-state and then underwent a hot restart. The acceptance thermal cycle was completed by continuing to operate QM1 after the hot restart at the full power condition until it once again achieved thermal steady-state temperatures.

In the final phase of acceptance hot fire testing, the performance of QM1 was assessed at all four of its nominal operating conditions: 600 V/9 kW, 600 V/10 kW, 600 V/11 kW, and 600 V/12 kW. The results of this performance assessment are shown in Table 1 and verified that QM1 met all AEPS requirements.

**Table 1** QM1 ATP performance results at nominal operating conditions

<b>Throttle Condition</b>	Thrust (mN)	Specific Impulse (s)
600 V/9 kW	444	2605
600 V/10 kW	491	2651
600 V/11 kW	540	2704
600 V/12 kW	586	2736
Uncertainty	± 5	± 25

Following acceptance hot fire, QM1 returned to AR's site in Redmond, Washington for a detailed set of functional tests, dimensional inspections, and mass measurements. The functional tests were identical to the ones performed immediately prior to the start of ATP and included photographic inspection, continuity and isolation resistance measurements, and a detailed magnetic field map. Taken together, these close out activities confirmed that QM1 still met all design requirements after being subjected to both acceptance vibration and hot fire testing and was therefore cleared to begin its qualification test campaign.

## 5.2 QM1 Thruster Qualification Testing

As discussed in Ref. [5], AEPS qualification activities are divided between two qualification model thrusters: QM1 is primarily dedicated to verifying design compliance to AEPS environmental requirements while QM2 is primarily dedicated to verifying AEPS lifetime requirements via a qualification wear test. An overview of the QM1 environmental QTP is shown in Fig. 8. QM1 QTP began in October 2023, and, as of the time of writing, the thruster has successfully completed all test phases through qualification shock. The following sections will summarize the results of the QTP test phases completed thus far.

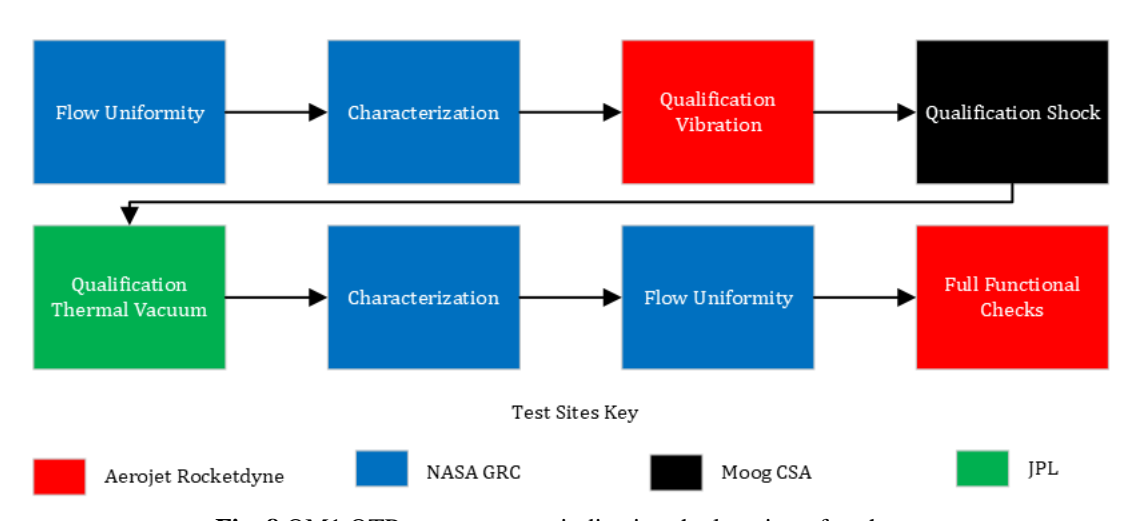
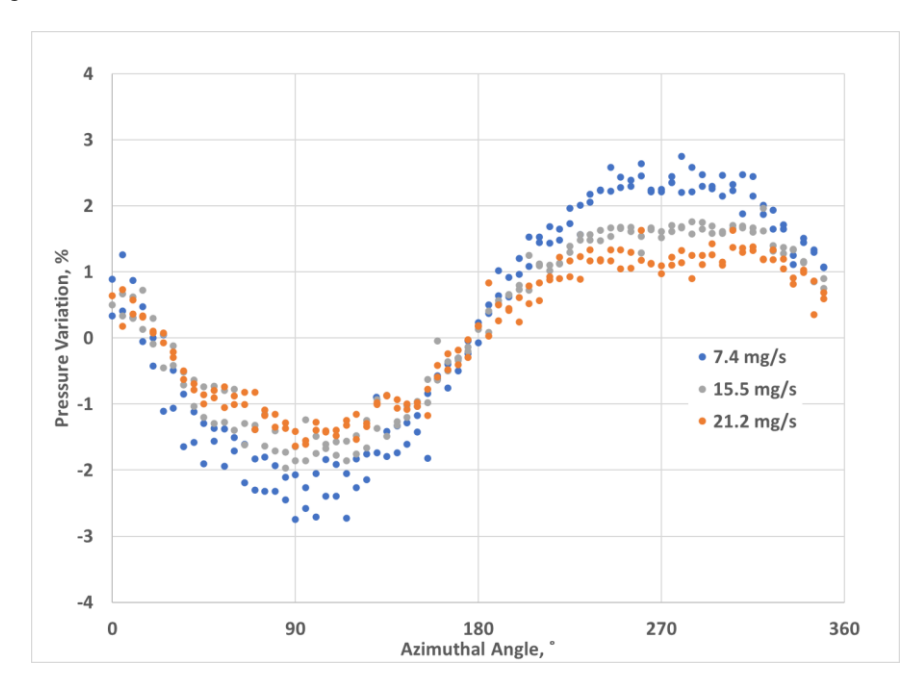


Fig. 8 QM1 QTP test sequence, indicating the location of each test

#### 5.2.1 Anode Flow Uniformity Testing

Propellant manifold (anode) flow uniformity testing of the QM1 thruster was performed at NASA GRC in VF-5. The test is performed to characterize the flow uniformity in the thruster's discharge channel at the start and end of the thruster's qualification test campaign to verify the anode still meets uniformity requirements after exposure to environments (see Fig. 8). A similar test is performed by AR at the sub-assembly level on all anodes to ensure uniform gas distribution prior to installation into the thruster assembly. In this test, pressure is measured as a proxy for the neutral density of the flow. The flow uniformity test entailed performing pressure measurements every 5° at the discharge channel centerline at the mid axial distance between the anode face and the exit plane of the thruster. Pressure measurements were made by insertion of a ¼" propellant tube that is coupled to an ion gauge. The pressure and ion gauge assembly was mounted on a rotary stage that rotates 350°. The flow uniformity of the QM1 thruster was characterized at anode flow rates of 7.4, 15.5, and 21.2 mg/s. Pressure readings were collected in the clockwise and counter-clockwise directions to evaluate pressure reading hysteresis. Figure 9 shows the average normalized azimuthal pressure variation for all three test

conditions. The results in Fig. 9 show that the pressure (flow) variation in the discharge channel is less than 3% for the 7.4 mg/s test. The data also show that flow uniformity improves with increased flow rate, with pressure variation being <2% at a flow rate of 21.2 mg/s (12 kW operation flow rate). The sinusoidal variation with angle seen in Fig. 9 has been observed in flow modeling performed by AR as well as measurements on other AEPS thrusters and is an artifact of the AEPS anode design.



**Fig. 9** Azimuthal average normalized pressure variation in the discharge channel of the QM1 HCT at 7.4, 15.5 and 21.2 mg/s xenon flow rate

#### 5.2.2 Pre-environmental Characterization Testing

Following anode flow uniformity testing, QM1 underwent a second hot-fire test sequence in VF-5 at NASA GRC. Unlike during ATP, the goal of this test was to perform a detailed characterization of thruster performance, stability, and plume properties across the full range of throttle conditions to establish a baseline against which the thruster can be compared following exposure to qualification-level mechanical and thermal environments. QM1 is shown installed in VF-5 in Fig. 10 prior to the start of the Pre-environmental Characterization Test.

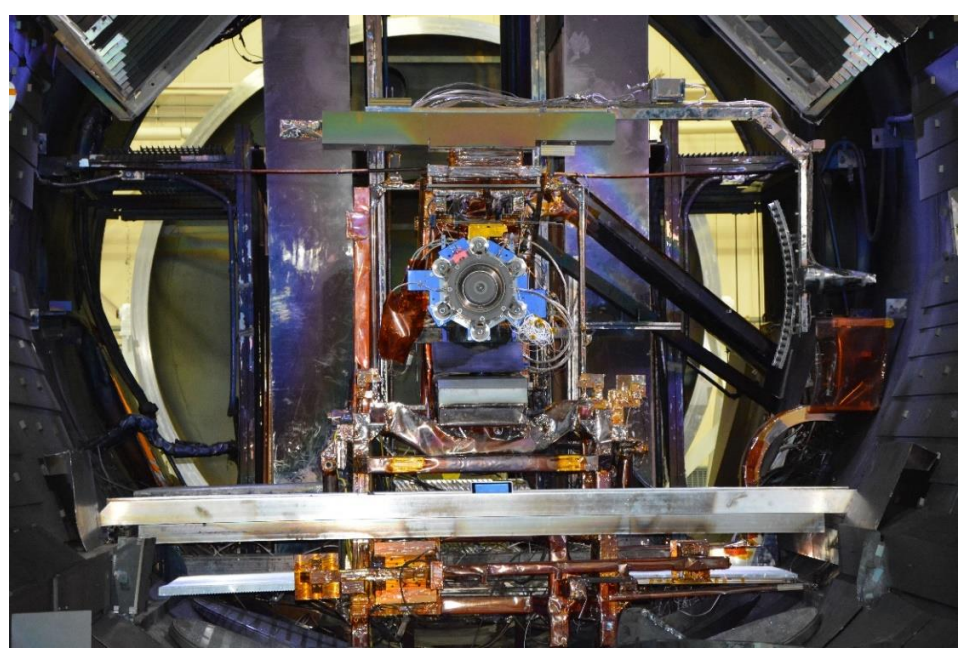


Fig. 10 QM1 installed in VF-5 prior to the start of the Pre-environmental Characterization Test

Following thruster conditioning, the performance of QM1 was assessed at all four of its nominal operating conditions using the same process as during ATP. Detailed maps of QM1 plume properties and thrust vector were then acquired at these same four operating conditions using the diagnostic package detailed in Refs. [6-7]. Example measurements of the QM1 thrust vector are shown in Fig. 11. Note that in Fig. 11, "Theta" refers to azimuthal angle (i.e., the angle in the horizontal plane) and "Phi" refers to the polar angle (i.e., the angle in the vertical plane).

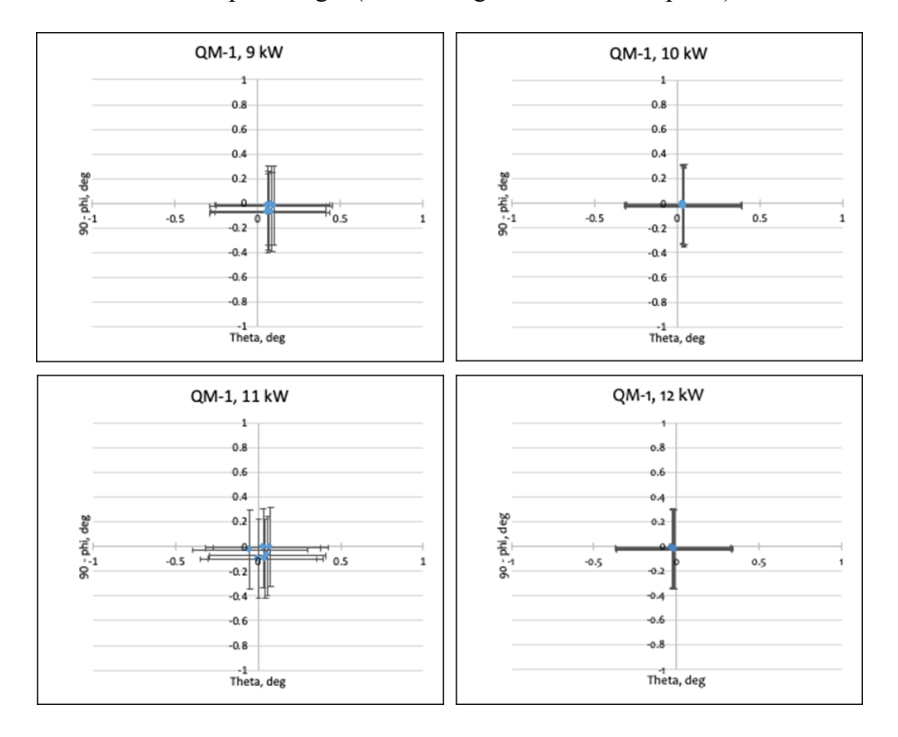


Fig. 11 Measurements of QM1 thrust vector acquired during Pre-environmental Characterization Testing

Following these assessments, a pair of sensitivity studies were conducted to ensure that the AEPS design can maintain stable operation across a range of input parameters. In the first of these sensitivity studies, thruster performance and stability were assessed as the discharge current was varied from 10-20 A at 300 V of operation and 14-20 A at 600 V of operation. The second sensitivity study assessed thruster performance, stability, and thermal properties as the coil currents supplied to the QM1 magnets were varied within the expected setpoint accuracy for application on PPE. In the final phase of the pre-environmental characterization test, QM1 was repeatedly cycled at the 600 V/12 kW condition until sufficient hours and cycles were achieved to simulate the worst-case values that could be accumulated on a flight unit prior to launch.

The QM1 Pre-environmental Characterization Test was completed in March 2024 and successfully established a detailed baseline of thruster performance, stability, and plume properties across the full range of throttle conditions. Except for thruster cycling, these test sequences will be identically repeated following qualification-level vibration, shock, and thermal vacuum testing to verify nominal operation and therefore demonstrate QM1 compliance with all AEPS environmental requirements.

# 5.2.3 Mechanical Environment Testing

The thruster Mechanical Environment Testing verifies the AEPS flight thruster design against the dynamic environmental requirements. This test sequence consisted of qualification-level vibration and shock tests. The vibration test included random and sinusoidal vibration environments for each orthogonal axis. A low-level sinusoidal vibration sweep was performed between each random and sinusoidal vibration. Similar to the acceptance dynamic test, electrical health checks and visual inspections were performed before and after vibration testing to verify no changes to the mechanical or electrical properties occurred. Data from these tests demonstrated that the thruster design has a resonance frequency higher than the minimum required value. Health functional checks indicated there were no changes in thruster characteristics after exposure to the vibration environment. At the time of writing, the thruster has completed shock testing at Moog CSA with results being analyzed, but health functional checks indicated no issues after exposure to the shock environment. Results from this test will demonstrate that the thruster shock isolators provide sufficient damping of the

anticipated shock events.

# 5.3 Cathode Qualification Testing

As part of the AEPS qualification test program, components that are susceptible to cyclic failure modes, such as the cathode, undergo component-level qualification tests to verify design compliance. In particular, these components undergo both thermal and operational life cycles as part of life verification. Prior to these cycles, the cathode is also subject to mechanical environment testing to verify design compliance to AEPS structural requirements. An overview of the cathode qualification test program is shown in Fig. 12. At the time of writing, the cathode had successfully completed Pre-environmental Characterization Testing and Mechanical Environment Testing. The following sections summarize the results of the completed test phases thus far.

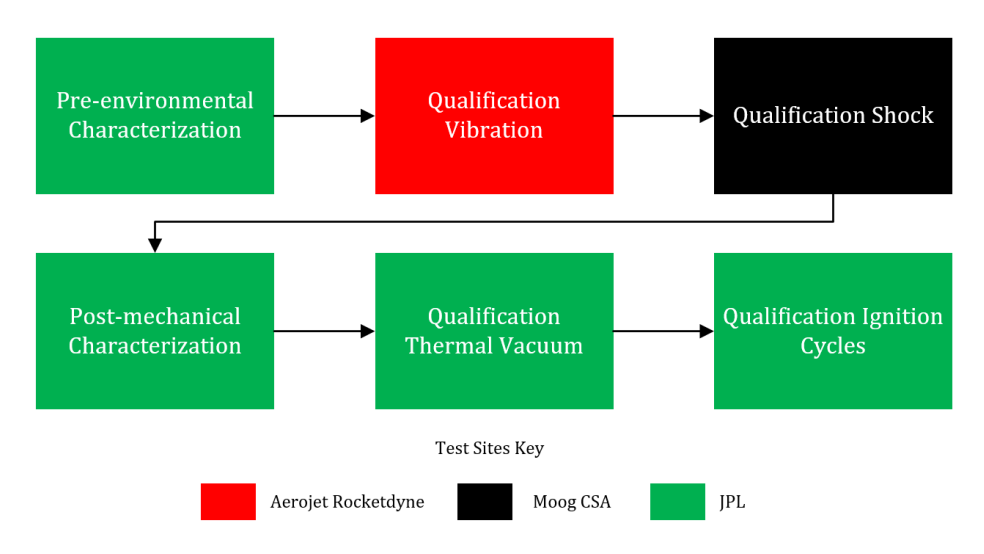


Fig. 12 Cathode qualification test sequence, indicating the location of each test

## 5.3.1 Pre-environmental Hot-Fire Testing

The qualification cathode assembly underwent initial hot-fire characterization at JPL in December 2023. This test served to establish a baseline characterization of cathode operational performance prior to mechanical, thermal, and cyclic environments. This included evaluating cathode telemetry over the range of operating set points required during thruster operation and an assessment of margin between cathode spot and plume modes.

Hot-fire testing began with conditioning the cathode to reduce the risk of emitter poisoning. Cathode conditioning consisted of incrementally increasing the cathode heater power to volatize and remove contaminants from the emitter surface, then igniting the cathode in keeper mode and extinguishing the cathode after confirmation of ignition. Following cathode conditioning, the cathode was ignited per the nominal thruster ignition sequence, then performance was assessed at all five of the thruster's nominal conditioning and operating set points (300 V/3 kW, 600 V/9 kW, 600 V/10 kW, 600 V/11 kW, and 600 V/12 kW). The facility DAQ records low-speed current and voltage telemetry for general monitoring of trends and verification of set point requirements. High-speed current and voltage telemetry are recorded for ignition and steady state operation on an oscilloscope to assess electrical performance. Both DAQ and oscilloscope data are reviewed to identify trends in cathode operational characteristics over the course of the qualification test.

Next, plume mode characterization was performed. The cathode was ignited and transitioned to the nominal 600 V/12 kW thruster set point, then the flowrate was incrementally reduced while maintaining constant discharge current until a transition to plume mode was observed. Transition to plume mode was defined as any observation of a sudden change in cathode plume visible properties, sudden change in discharge voltage, sudden increase in peak-to-peak discharge voltage or keeper to cathode peak-to-peak oscillations. Plume mode was not observed until the flowrate was 25% of the nominal, demonstrating significant margin between spot and plume modes. All four criteria of a transition to plume mode were observed at this flowrate.

After completion of plume mode characterization, keeper mode characteristic testing was performed. This portion of characterization testing evaluated cathode ignition and keeper mode characteristics across the envelope of allowable flowrates and heater powers permitted per thruster requirements. This test consisted of igniting the cathode in keeper mode at various combinations of flowrates and heater currents. All ignitions attempted in this test were successful with stable electrical telemetry, demonstrating that the design is robust across the operational envelope.

Similar hot-fire characterization tests will be performed periodically throughout the qualification test campaign to evaluate the evolution of cathode operating characteristics during the course of the test.

## 5.3.2 Mechanical Environment Testing

Once pre-environmental hot-fire testing was complete, the cathode underwent qualification-level vibration testing at AR's site in Redmond, Washington. For vibration testing, the cathode was installed into a thruster dynamic mass simulator, a tooling fixture representative of the thruster's mass characteristics. This ensured the mechanical loads delivered to the cathode during these tests were consistent with expected loads for the flight design thruster. The cathode was subjected to the same vibration tests (random, sinusoidal, low-level sinusoidal sweeps) in all three axes as the thruster QTP. An image of the cathode vibration test configured for X-axis is shown in Fig. 13.

Following vibration testing, the cathode was delivered to Moog CSA in Mountain View, California for qualification-level shock testing. Similar to vibration testing, the cathode was installed into a thruster dynamic mass simulator for this test. The shock test consisted of performing two AEPS qualification-level shock hits in each of the three axes. Qualification-level cathode vibration and shock tests were both completed in accordance with the AEPS requirements, demonstrating both AR and Moog CSA's facilities were qualified for qualification-level thruster testing.

Both prior to and following vibration and shock tests, a collection of electrical health checks (e.g., continuity and isolation resistance), visual inspections, and dimensional inspections were conducted. These served to evaluate electrical health and identify changes in the cathode as it is processed through the qualification test program. Results from these tests and inspections indicated no discernable change in structural or electrical characteristics following exposure to vibration and shock environments. This suggests that the cathode design is compliant to AEPS structural requirements, however, full verification of cathode structural requirements will not be made until the cathode has successfully completed TVAC and Ignition Cycles tests. Electrical health checks will continue to be made at periodic stages of the TVAC and Ignition Cycles tests. At the time of writing, the cathode is preparing for post-mechanical characterization testing at JPL.

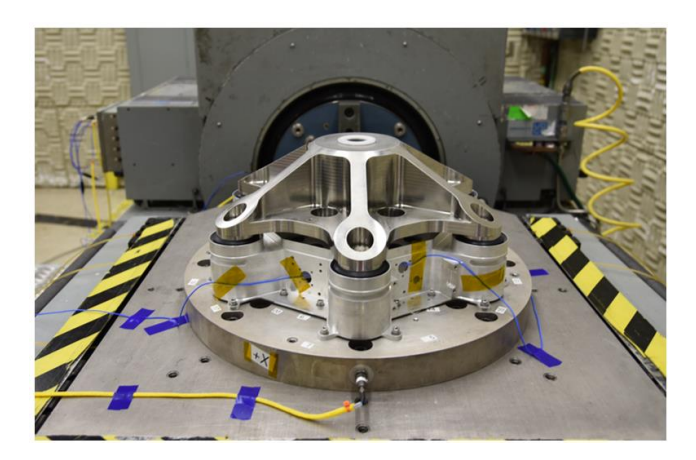


Fig. 13 Cathode Qualification Vibration Test setup, including the thruster dynamic mass simulator

## 5.4 Component Qualification Testing

In parallel with thruster- and cathode-level testing, the AEPS project is performing a ground qualification of mission-critical components. Testing at the component level has the benefit of allowing data collection on multiple units without the complexity of performing a test at the thruster level. Further, the thermal vacuum and life cycle test parameters are controlled much more precisely for the individual components than if the testing were relying on typical TVAC test methods such as radiative heating. Thruster subassemblies and components were selected based on their margin to the expected thermal environments and the consequence of that component's failure. The cathode heater, inner and outer magnets, and thermal components, which are comprised of the magnet heaters, heater transition tubes, and Resistive Temperature Detectors (RTDs), were selected to undergo component-level cycle testing.

All components are being tested at the Component Test Facility (CTF) at NASA JPL. The CTF has been equipped with custom thermal cycling fixtures which are used to facilitate multiple component tests simultaneously. All component tests follow the same QTP sequence outlined in Fig. 14. At the time of writing, component testing had commenced on the magnet coils and thermal components. At the beginning of each test, each component received a full electrical and visual functional checkout to verify compliance to beginning of life requirements and record the test article characteristics. Once installed in the CTF, the components were subjected to a thermal vacuum (TVAC) test per SMC-S-016 [8].

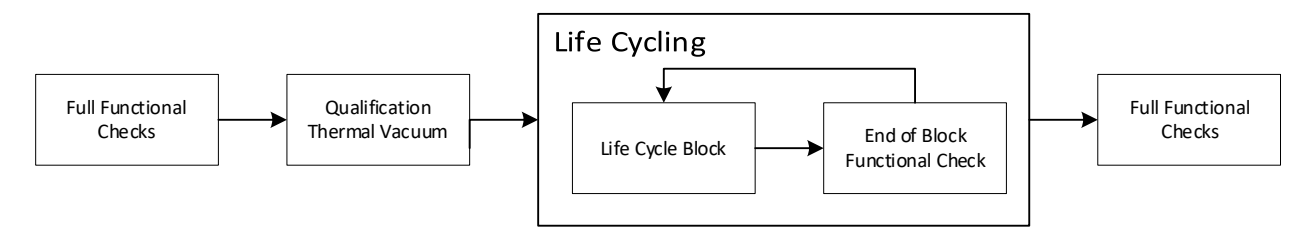


Fig. 14 Component qualification test sequence

After completion of the TVAC cycles, the components began their life cycle testing. This testing is still in progress for all components undergoing QTP. During life cycling, the components are operated while being driven to the worst-case hot and cold temperatures expected during the mission profile. However, unlike the TVAC cycles there are no dwell or soak requirements once the components achieve the worst-case temperatures. All components will be tested to 1.5 times the thruster life cycle requirement. Given the extended duration of life cycle testing, the cycles have been divided into life cycle blocks. Following each block, trends in the data are reviewed and the components undergo abbreviated functional testing while still installed in the CTF and under vacuum. Once the components have completed the full duration of life cycle testing, they will be uninstalled, visually examined, and will undergo a complete end-of-life functional checkout.

#### 6.0 NASA Risk Reduction and Characterization Tests for AEPS

In addition to qualification testing led by AR, several tests have been conducted by NASA in support of AEPS characterization and risk reduction. These include integration tests such as characterization of the radiation emissions (RE) EMI from the AEPS thruster, development testing on the HERMeS TDU-2 thruster to validate erosion mechanisms which are captured in the AEPS thruster lifetime models, and characterization of the impacts of extended atmospheric exposure on AEPS hollow cathodes. The status of each of these tests is summarized below.

## 6.1 EMI Characterization of the AEPS Thruster

As part of the AEPS thruster qualification, the AEPS ETU-2 thruster RE EMI were characterized at The Aerospace Corporation (TAC) EP3 facility. TAC's EP3 vacuum chamber main volume is 4 m diameter and is 9 m long, with a conically-shaped fiberglass extension (largely transparent to radio frequency waves) attached to the main volume. The 8 ft-long fiberglass port is enclosed within a semi-anechoic room that includes hybrid absorber treatment that meets MIL-STD-461G standards for reflectivity including frequency coverage from 10 kHz - 40 GHz. For the AEPS EMI test campaign, the thruster was powered with Maxar's PPU and xenon flow was fed with Moog 's XFC. This was done to incorporate string-level interactions in the test and for Maxar to gain more experience with integrated AEPS operation. For this test campaign, the thruster was mounted in the conical fiberglass section. Figure 15 shows a photograph of the ETU-2 thruster mounted inside TAC's EP3 fiberglass conical port. Initial test activities included performing xenon feed system bakeout, thruster magnet conditioning, cathode conditioning, and thruster conditioning. After initial activities were completed, EMI characterization of the thruster was performed.

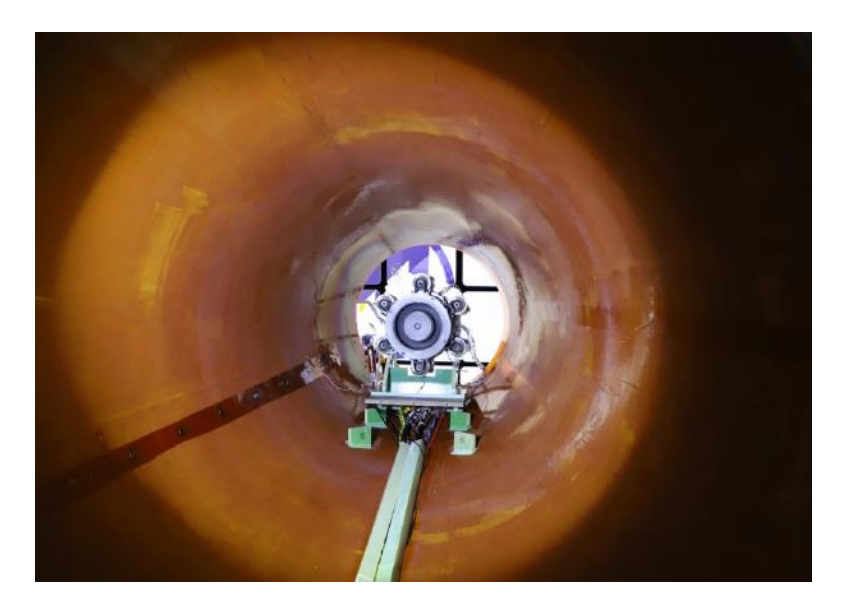


Fig. 15 Photograph of the AEPS ETU-2 HCT inside TAC's fiberglass conical port

For the EMI test campaign, tests were performed at power levels from 3 to 12 kW at discharge voltages of 300 and 600V. Figure 16 shows a photograph of the thruster while operating at 12 kW. During the entire test campaign, the pressure and thermal environments within the fiberglass chamber were well within acceptable ranges for nominal thruster operation – the ratio of discharge current-to-flow rate and discharge current ripple were similar to what was observed during operation in NASA GRC's Vacuum Facility 6. RE-102 and extended RE-102 frequency domain characterization of the ETU-2 radiated emissions were completed from 10 kHz to 40 GHz. This included acquiring data at:

- 1. Five antenna locations with horizontal and vertical polarizations, with evaluation performed at select antenna locations;
- 2. Different thruster throttle conditions; and
- 3. Select off-nominal and transient thruster operations.

Time domain characterization studies were also performed for select frequency bands of interest. Different time domain methods were employed including real time spectrum analysis, zero-span dwells, and broadband direct noise characterization. The RE test campaign was successful with all the primary and secondary objectives met. At the time of this writing, the test data is being processed and further assessed. The test campaign also demonstrated TAC's new EP3 vacuum facility capability to accommodate operation of higher power Hall thrusters and demonstrated the reconstitution of TAC's RE measurement capability.

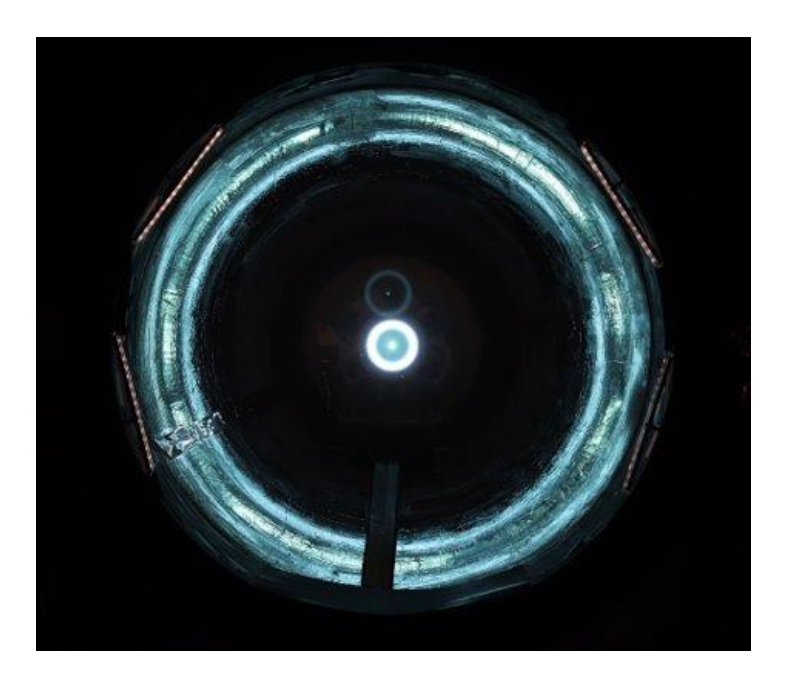


Fig. 16 Photograph of the AEPS ETU-2 HCT operating at full power inside TAC's fiberglass conical port

# **6.2 AEPS Lifetime Model Anchoring Tests**

Qualification of the AEPS thruster for a 23,000-hour operational life will be accomplished through a 23,000-hour wear test at GRC, with 1.5x life margin [9] to be demonstrated by plasma modeling of erosion processes with the Hall2De [10-11] and OrCa2D [12] codes. In order to build sufficient confidence in the models, detailed validation of the simulated spatially and temporally resolved plasma properties is required, going beyond comparisons of global performance metrics and erosion rates. Throughout the AEPS project, non-perturbing laser-induced fluorescence (LIF) measurements of local ion velocities have been the primary source of high-fidelity validation data [13-17] enabling important advances in the physics captured by the models [10] and ensuring reliable calibration of the non-classical cross-field electron transport, which is currently implemented in Hall2De through an empirical anomalous collision frequency [18].

Motivated in part by LIF measurements of counter-streaming ions in front of the inner pole [13], recent theoretical developments [19-20] predicted that microturbulence associated with unstable waves in the lower hybrid frequency range could produce the extra ion heating needed to explain measured pole cover erosion rates in the AEPS thruster [21]. As a first step toward validating these predictions, an LIF campaign was undertaken at JPL in 2022-2023, using the HERMeS TDU-2 test article, with objectives to study mean ion velocities and ion heating in the r-z plane and, for the first time in AEPS, in the azimuthal direction. Comparing ion energy spreads along different directions can provide evidence for the relative importance of different heating mechanisms; for example, lower hybrid wave heating can occur in the r-z plane along the direction approximately perpendicular to the magnetic field through the modified two-stream instability (MTSI) [19], or in the azimuthal direction through the lower hybrid drift instability (LHDI) [20].

The new azimuthal ion velocity results are presented in detail in Ref. [22]. Throughout the cathode plume, near pole regions, and main beam, the measured ion velocity distribution functions (IVDFs) were typically fit well by a bi-Maxwellian function of the form  $f_{i\theta}(v) = A_1 \exp\left(-\frac{(v-u_{\theta 1})^2}{v_{T\theta 1}^2}\right) + A_2 \exp\left(-\frac{(v-u_{\theta 2})^2}{v_{T\theta 2}^2}\right)$ . Noting that two distinct thermal ion populations may not actually have been present in many cases, we quantify the ion energy spread by defining an effective azimuthal ion temperature:

$$T_{i\theta,eff} \equiv \frac{m_i}{k_B} \left( \frac{\int (v - u_\theta)^2 f_{i\theta}(v) dv}{\int f_{i\theta}(v) dv} \right) \tag{1}$$

where  $u_{\theta} \equiv (A_1 v_{T\theta 1} u_{\theta 1} + A_2 v_{T\theta 2} u_{\theta 2})/(A_1 v_{T\theta 1} + A_2 v_{T\theta 2})$  is the overall mean ion velocity.

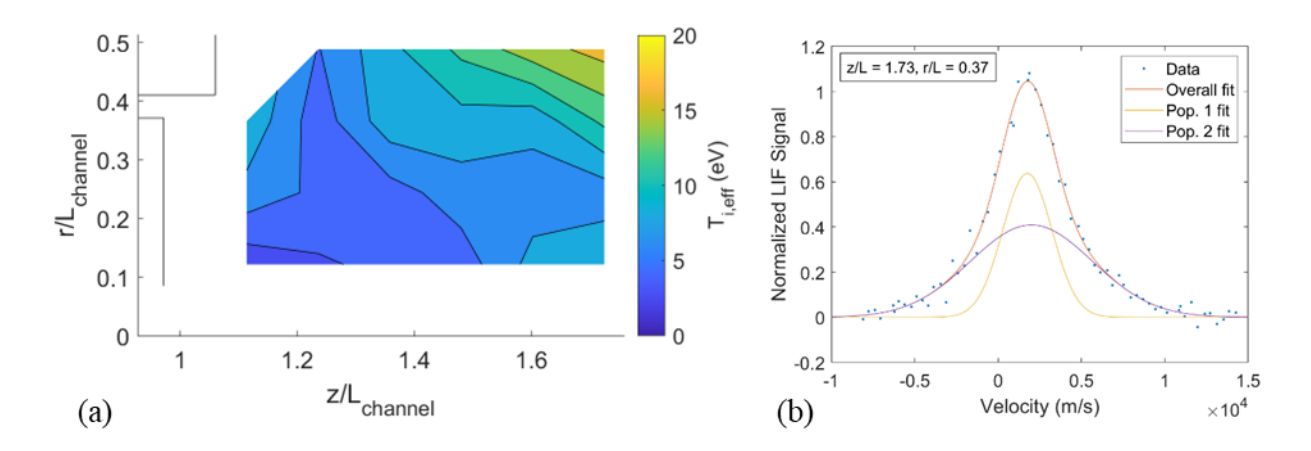


**Fig. 17** (a) Effective azimuthal ion temperature in the cathode plume at the 600 V, 12 kW operating condition with nominal magnetic field strength. (b) Example of raw LIF data and bi-Maxwellian fit at  $z/L_{channel} = 1.73$ ,  $r/L_{channel} = 0.37$ 

Figure 17 presents an example of azimuthal ion energy spread data in the cathode plume. The effective temperature is low near the keeper orifice but increases moving away axially and radially, with a typical value of 5-10 eV throughout most of the cathode plume (roughly comparable to the ion energy spread in the r-z plane [15], and also at least as large as the expected electron temperature at this location [12]). Figure 17b shows that the IVDF at  $z/L_{channel} = 1.73$ ,

 $r/L_{channel} = 0.37$  has broad positive and negative tails, allowing it to be fit by a sum of cool and warm Maxwellians with similar mean velocities. Qualitatively similar IVDFs were obtained within the main beam.

On the channel centerline, the ions were rapidly heated in the azimuthal direction in the region from  $z/L_{channel} = 1.05-1.45$  (just downstream of the peak axial electric field [16]), as shown in Fig. 18. The classical ion collision mean free path for beam ions at this location is much longer than  $L_{channel}$ , and axial LIF measurements show that the azimuthally heated population cannot be solely composed of axially "slow" ions born downstream of the acceleration region [17]. Therefore, heating by low-frequency (e.g., spoke mode) or high-frequency (e.g. lower hybrid modes) waves is the most likely explanation. More discussion of these results and others is presented in Ref. [22], while details of the recent efforts and results of erosion modeling using Hall2De can be found in Refs. [23-24].

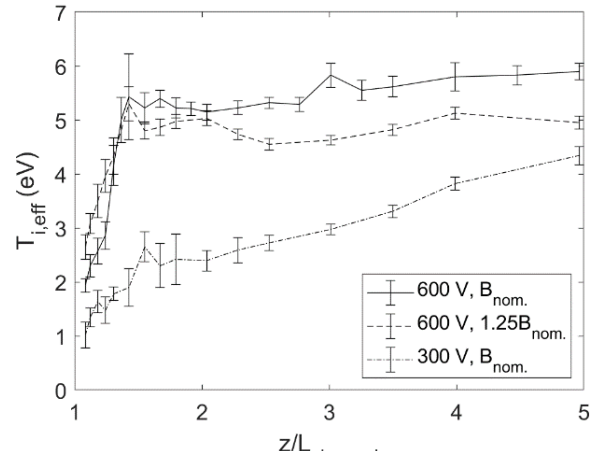


**Fig. 18** Effective azimuthal ion temperature along the channel centerline at three operating conditions

## 6.3 Impact Characterization from Extended Atmospheric Exposure on AEPS Cathodes

A critical component of the AEPS thruster is a centrally-mounted hollow cathode, which generates the charged particles necessary for efficient operation of the thruster. Earlier testing [25] was performed with NASA-built cathodes to demonstrate capability. Subsequently, an Engineering Development series of cathodes were fabricated by AR, which has also been used to demonstrate design capability. AR built three Engineering Development Unit (EDU) cathodes, with the third one delivered to NASA GRC for risk reduction activities.

While the plan for the Engineering Development Unit-3 (EDU-3) cathode test campaign began as a cathode test to address risk of life capability against AEPS requirements, it has since evolved to address the additional risk of future missions requiring extended allowable atmospheric exposure durations prior to launch. As such, NASA developed a test campaign to expose EDU-3 to extended durations of worst-case atmospheric conditions and characterize any impacts on cathode performance and lifetime. The process flow of the EDU-3 cathode test campaign is shown in Fig. 19. Currently the EDU-3 cathode has completed the post-exposure characterization and next it will undergo physical characterization (red box in Fig. 19) prior to starting the long duration wear test campaign. While there were several test anomalies that arose during the test campaign to-date, EDU-3 cathode performance has been fully successful with no signs of negative impacts from extended exposure. In addition, the first keeper-only ignition was successful with the ignition break down

occurring on the first ignitor pulse.

The EDU-3 cathode has accumulated a total of 4618 hours of exposure; 1504 hours are from the pre-activation environmental exposure; 3020 hours are from the post-activation environmental exposure; and the remainder from handling and storage. The exposure of the cathode was accumulated within an environmental chamber set to the conditions of 35 °C temperature with a relative humidity of 20%, which resulted in a dew point of 15 °C.

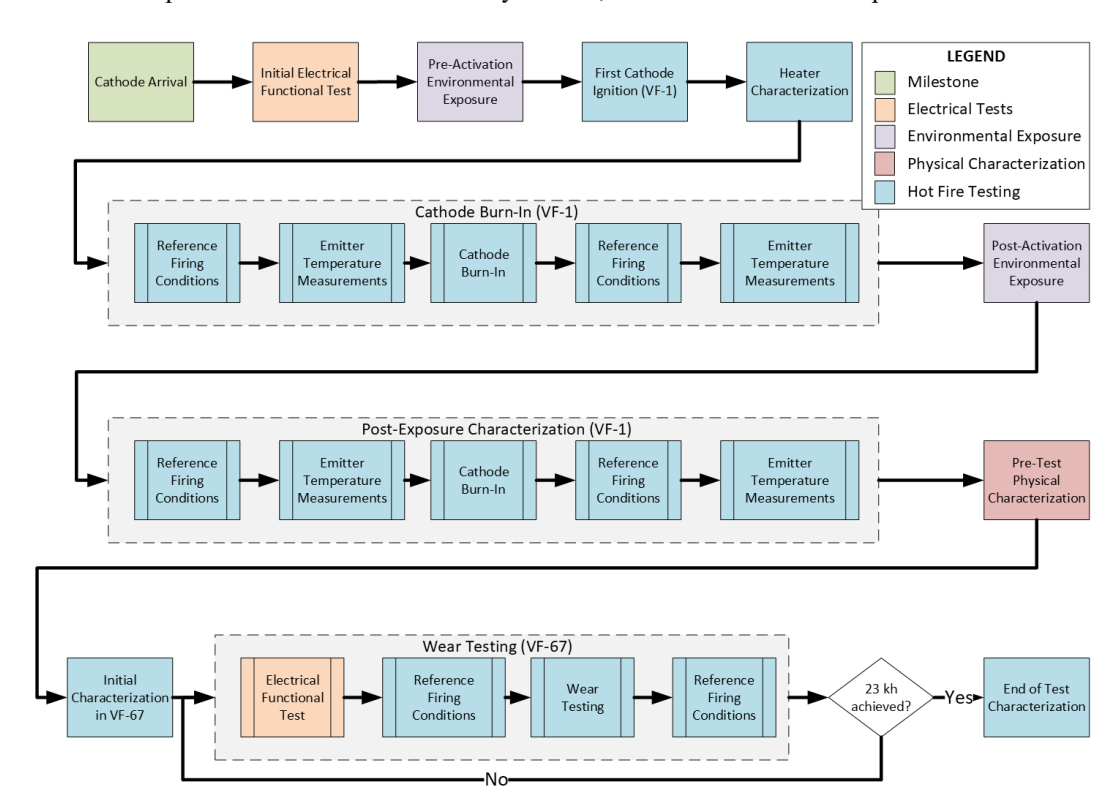


Fig. 19 Planned EDU-3 test sequence flow

The pre- and post-exposure characterization consisted of operating the cathode over a set of reference firing conditions (varying discharge current, xenon flow rate, and with and without a magnetic field simulator active); measuring emitter surface temperatures; and operating the cathode at the nominal wear condition without the magnetic field for durations representing worst case ground acceptance testing. These reference firing conditions are derived from the AEPS thruster setpoints. Additionally, a plume mode detection sweep is performed by decreasing the flowrate at a constant discharge current and monitoring the change in discharge voltage. Plume mode was not observed, but there was evidence that the cathode was starting to transition out of spot mode at the lowest tested flowrate. The plume mode sweep provides indirect indications of cathode orifice erosion. The emitter temperature profiles and reference firing conditions showed little variation between pre and post characterization, suggesting that the cathode, during early operation, is insensitive to the extended atmospheric exposure. Findings on this behavior will be detailed in a future publication.

## 7.0 Summary

The AEPS contract was awarded to AR in 2016 with the goal of developing and fully qualifying a 12 kW Hall thruster for NASA and commercial applications, with its first intended use on the Power and Propulsion Element as part of NASA's Gateway lunar space station. The thruster design successfully passed CDR in 2022, with qualification activities and flight hardware fabrication underway. To-date, the QM1 qualification thruster has successfully undergone preenvironmental characterization testing, qualification vibration and shock testing, with preparations for TVAC testing underway at time of writing. Additional qualification testing of components such as the cathode, magnet coils, and thermal components are ongoing to demonstrate design robustness of these critical thruster elements. In its insight/oversight role, NASA has also conducted numerous risk reduction tests in support of AR's qualification campaign and the PPE mission. Flight hardware fabrication and testing is expected to be completed by 2025, at which point the hardware will be delivered to Maxar Technologies for integration and use on the PPE spacecraft.

### References

- [1] Soendker, E., Jackson, J., Branch, N., Poehls, A., and Simon, G., "Aerojet Rocketdyne Robust PPU Development Testing and Integrated System Hot Fire", 71st JANNAF Propulsion Meeting, Oklahoma City, OK, May 6-10, 2024.
- [2] Frieman, J. D., Kamhawi, H., Peterson, P. Y., Herman, D. A., Gilland, J. H., and Hofer, R. R., "Completion of the Long Duration Wear Test of the NASA HERMeS Hall Thruster", *AIAA Propulsion and Energy 2019 Forum*, AIAA-2019-3895, Indianapolis, IN, August 19-22, 2019.
- [3] Frieman, J. D., Kamhawi, H., Huang, W., Mackey, J., Ahern, D. M., Peterson, P. Y., Gilland, J. H., Hall, S. J., Hofer, R. R., Inaba, D., Dao, H., Zubair, J., Neuhoff, J., and Branch, N., "Characterization Test of the 12.5-kW Advanced Electric Propulsion System Engineering Test Unit Hall Thruster", *AIAA Propulsion and Energy 2020 Forum*, AIAA-2020-3626, Virtual Event, August 24-28, 2020.
- [4] Frieman, J. D., Kamhawi, H., Mackey, J., Peterson, P. Y., Hofer, R. R., Inaba, D., Dao, H., Branch, N., and Welander, B., "Extended Performance Characterization of the 12.5-kW Advanced Electric Propulsion System Engineering Test Unit Hall Thruster", AIAA Propulsion and Energy 2021 Forum, AIAA-2021-3431, Virtual Event, August 9-11, 2021.
- [5] Jackson, J., Miller, S., Cassady, J., Soendker, E., Welander, B., Barber, M., and Peterson, P., "13 kW Advanced Electric Propulsion Flight System Development and Qualification", *36th International Electric Propulsion Conference*, Vienna, Austria, September 15-20, 2019.
- [6] Benavides, G. F., Mackey, J. A., Ahern, D. M., and Thomas, R. E., "Diagnostic for Verifying the Thrust Vector Requirement of the AEPS Hall-Effect Thruster and Comparison to the NEXT-C Thrust Vector Diagnostic", 2018 Joint Propulsion Conference, AIAA-2018-4514, Cincinnati, OH, July 9-11, 2018.
- [7] Huang, W., Kamhawi, H., Haag, T. W., Lopez Ortega, A., and Mikellides, I. G., "Facility Effect Characterization Test of NASA's HERMeS Hall Thruster", *52nd AIAA/SAE/ASEE Joint Propulsion Conference*, AIAA-2016-4828, Salt Lake City, UT, July 25-27, 2016.
- [8] Space and Missile Systems Center, "Test Requirements for Launch, Upper-Stage and Space Vehicles." 2014.
- [9] Polk, J. E., and Brophy, J. R., "Life Qualification of Hall Thrusters by Analysis and Test", *Space Propulsion Conference*, Paper No 547, Seville, Spain, May 14-18, 2018.
- [10] Lopez Ortega, A., Mikellides, I. G., Chaplin, V. H., Huang, W., and Frieman, J. D., "Anomalous Ion Heating and Pole Erosion in the 12.5-kW Hall Effect Rocket with Magnetic Shielding (HERMeS)", *AIAA Propulsion and Energy Forum*, AIAA-2020-3620, Virtual Event, August 24-28, 2020.
- [11] Mikellides, I. G., and Katz, I. "Numerical simulations of Hall-effect plasma accelerators on a magnetic-field-aligned mesh," *Physical Review E* Vol. 86, 2012, p. 046703.
- [12] Mikellides, I. G., Katz, I., Goebel, D. M., and Jameson, K. K. "Evidence of nonclassical plasma transport in hollow cathodes for electric propulsion," *Journal of Applied Physics* Vol. 101, No. 6, 2007, p. 063301.
- [13] Huang, W., and Kamhawi, H. "Counterstreaming ions at the inner pole of a magnetically shielded Hall thruster," *Journal of Applied Physics* Vol. 129, No. 4, 2021, p. 043305.
- [14] Chaplin, V. H., Lobbia, R. B., Lopez Ortega, A., Mikellides, I. G., Hofer, R. R., Polk, J. E., and Friss, A. J. "Time-resolved ion velocity measurements in a high-power Hall thruster using laser-induced fluorescence with transfer function averaging," *Applied Physics Letters* Vol. 116, No. 23, 2020, p. 234107.
- [15] Chaplin, V. H., Lobbia, R. B., Lopez Ortega, A., Mikellides, I., Friss, A. J., Roberts, P. J., Peter, J. S., Hofer, R. R., and Polk, J. E., "Spatiotemporally Resolved Ion Velocity Distribution Measurements in the 12.5 kW HERMeS Hall Thruster", *36th International Electric Propulsion Conference*, IEPC-2019-532, Vienna, Austria, September 15-20, 2019.
- [16] Huang, W., Frieman, J. D., Kamhawi, H., Peterson, P. Y., and Hofer, R. R., "Ion Velocity Characterization of the 12.5-kW Advanced Electric Propulsion System Engineering Hall Thruster", *AIAA Propulsion and Energy Forum*, AIAA-2021-3432, Virtual Event, August 9-11, 2021.
- [17] Chaplin, V. H., Jorns, B. A., Lopez Ortega, A., Mikellides, I. G., Conversano, R. W., Lobbia, R. B., and Hofer, R. R. "Laser-induced fluorescence measurements of acceleration zone scaling in the 12.5 kW HERMeS Hall thruster," *Journal of Applied Physics* Vol. 124, No. 18, 2018, p. 183302.
- [18] Mikellides, I. G., and Lopez Ortega, A. "Challenges in the development and verification of first-principles models in Hall-effect thruster simulations that are based on anomalous resistivity and generalized Ohm's law," *Plasma Sources Science and Technology* Vol. 28, No. 1, 2019, p. 014003.
- [19] Mikellides, I. G., and Lopez Ortega, A. "Growth of the modified two-stream instability in the plume of a magnetically shielded Hall thruster," *Physics of Plasmas* Vol. 27, No. 10, 2020, p. 100701.
- [20] Mikellides, I. G., and Lopez Ortega, A. "Growth of the lower hybrid drift instability in the plume of a magnetically shielded Hall thruster," *Journal of Applied Physics* Vol. 129, No. 19, 2021, p. 193301.
- [21] Frieman, J. D., Gilland, J. H., Kamhawi, H., Mackey, J., Williams Jr., G. J., Hofer, R. R., and Peterson, P. Y.

- "Wear trends of the 12.5 kW HERMeS Hall thruster," *Journal of Applied Physics* Vol. 130, No. 14, 2021, p. 143303.
- [22] Chaplin, V. H., Byrne, M. P., Lobbia, R. B., Polk, J. E., Lopez Ortega, A., and Mikellides, I. G., "Azimuthal Ion Velocity Measurements in the 12 kW HERMeS Hall Thruster", *38th International Electric Propulsion Conference*, Toulouse, France, June 23-28, 2024.
- [23] Ortega, A. L., and Mikellides, I. G., "Validation of Hall2De simulations with anomalous ion heating in the pole region of a magnetically shielded Hall thruster", *37th International Electric Propulsion Conference*, IEPC-2022-299, Cambridge, MA, June 19-23, 2022.
- [24] Ortega, A. L., and Mikellides, I. G., "Erosion Mechanisms at the Outer Front Pole Cover of a Magnetically Shielded Hall Thruster", *38th International Electric Propulsion Conference*, IEPC-2024-264, Toulouse, France, June 23-28, 2024.
- [25] Peterson, P. Y., Herman, D. A., Kamhawi, H., Frieman, J. D., Huang, W., Verhey, T., Dinca, D., Boomer, K., Pinero, L., Criswell, K., Hall, S. J., Birchenough, A., Gilland, J. H., Hofer, R., Polk, J. E., Chaplin, V., Lobbia, R., Garner, C. E., and Kowalkowski, M. K., "Overview of NASA's Solar Electric Propulsion Project", 36th International Electric Propulsion Conference, IEPC-2019-836, Vienna, Austria, September 15-20, 2019.